Journal of Applied Polymer Science

Facile fabrication of polyethylene/silver nanoparticle nanocomposites with silver nanoparticles traps and holds early antibacterial effect

Dau Hung Anh,[1] Kanchana Dumri,[2,3] Nguyen Tuan Anh,[4] Winita Punyodom,[2,3] Pornchai Rachtanapun[1,3]

[1]Division of Packaging Technology, Faculty of Agro-Industry, Chiang Mai University, Chiang Mai 50100, Thailand
[2]Department of Chemistry, Faculty of Science, Chiang Mai University, Chiang Mai 50200, Thailand
[3]Materials Science Research Center, Faculty of Science, Chiang Mai University, Chiang Mai 50200, Thailand
[4]Microanalysis Department, Institute for Tropical Technology, Vietnam Academy of Science and Technology, Hanoi, Vietnam
Correspondence to: P. Rachtanapun (E-mail: pornchai.r@cmu.ac.th)

ABSTRACT: Antibacterial polyethylene (PE)/silver nanoparticle (AgNP) nanocomposites containing AgNPs at concentrations of 5×10^{-5}, 5×10^{-4}, and 5×10^{-3} wt % were fabricated and tested. Transmission electron microscopy revealed an even dispersion of surface AgNPs in the PE/AgNP nanocomposites. No AgNP agglomeration was observed. The tensile strength, elongation at break, and Young's modulus of these PE/AgNP nanocomposites were similar to those of neat PE. Differential scanning calorimetry demonstrated that the PE/AgNP nanocomposites and neat PE had similar melting and crystallization temperatures of 126 ± 0.5 and 109 ± 0.6°C, respectively. The heats of fusion of the PE/AgNP nanocomposites containing AgNPs at concentrations of 5×10^{-5} and 5×10^{-4} and of 5×10^{-3} wt % were lower than those of neat PE by 5 and 7%, respectively. These PE/AgNP nanocomposites were immersed in shaking liquid cultures of the potential pathogenic bacteria *Escherichia coli, Bacillus subtilis*, and *Salmonella typhimurium* in the lag phase. The results show that the growth rates of all of the tested bacteria were restricted effectively after 1.5, 3, and 6 h of cultivation, respectively. © 2016 Wiley Periodicals, Inc. J. Appl. Polym. Sci. **2016**, *133*, 43331.

KEYWORDS: antibacterial; nanocomposite; nanoparticle; packaging; polyethylene

Received 25 May 2015; accepted 9 December 2015
DOI: 10.1002/app.43331

INTRODUCTION

Silver nanoparticles (AgNPs) contained in polymer nanocomposites have been widely investigated to improve health care with their antibacterial properties in a variety of polymers.[1,2] The antibacterial packaging that can be made from these materials may contribute as promisingly powerful tools for alternative community health care by early prevention of many occasionally pathogenic bacteria in several regions, for example, South East Asia, where people have face anomalous disasters, such as drought or flooding, that can lead to certain serious plagues via the contaminated environment.[3–7] AgNPs have been reported to kill pathogenic bacteria through the release of Ag^+ ions; this may inhibit bacterial cell processes and gene expression,[8–10] but usefully, they are not hazardous to human cells.[11,12] The incorporation of AgNPs in polymers such as plastics [e.g., polyethylene (PE),[13] polypropylene (PP), polystyrene,[14] and poly(vinyl chloride)[15]] to form nanocomposites is always interesting because of their possible antibacterial activity in combination with the mechanical properties of conventional plastics.[16] Various silver nanocomposites have been reported as suitable for antimicrobial packaging.[17,18] However, the development of techniques for producing AgNPs with enhanced antibacterial activity with the aim of mass production in some countries is still challenging. There are three basic methods for producing nanocomposites: (1) melt compounding, (2) solution blending, and (3) *in situ* polymerization.[19] Melt compounding is suitable for producing PE or PP silver nanocomposites with raw high-density polyethylene (HDPE)[20] and low-density polyethylene (LDPE)[18] or PP materials[21] in which the final nanocomposites will be produced by compression-molding equipment. A bottleneck for this type of silver nanocomposite production is the introduction of AgNPs into the PE or PP matrix. This influences the antibacterial activity of the nanocomposites and is critical. AgNPs can be first immobilized on SiO_2 or TiO_2 to form colloidal SiO_2/AgNPs and TiO_2/AgNPs, and then, these are mixed with LDPE granules to form AgNPs/PE nanocomposites after melting/blending.[18] In case of an AgNPs/PP nanocomposites, the colloidal AgNP solution is diluted with ethanol and directly mixed with PP granules and extruded to give the product.[21] A common feature of these AgNP nanocomposites is

Figure 1. (a) AgNP traps in a round aluminum mold, (b) specimens of a PE/AgNP disc (left side) and PE/AgNP squares for antibacterial testing (right side), and (c) mixed tested bacterial cultures with PE/AgNP nanocomposites. [Color figure can be viewed in the online issue, which is available at wileyonlinelibrary.com.]

that the agglomeration of AgNPs release fewer Ag^+ ions than when the AgNPs remain separate.[22,23] Hence, this can reduce the antibacterial properties of these products. Therefore, we propose a new technique for incorporating AgNPs into the PE matrix. AgNPs with sizes from 2 to 20 nm were first captured in a dry disc trap based on PE. The dishes were ground into a mild powder and mixed with massive PE granules for melt/blending to form PE/AgNP nanocomposites. The presence of AgNPs on these PE/AgNP nanocomposites, the tensile properties, and the melting temperature (T_m) and crystallization temperature (T_c) values were investigated. Antibacterial activity tests with the potentially pathogenic bacteria *Escherichia coli, Bacillus subtilis*, and *Salmonella typhimurium* in liquid cultures were performed, and effective bacterial growth restriction was observed.

EXPERIMENTAL

Materials

Chemicals. Silver nitrate ($AgNO_3$), sodium borohydride ($NaBH_4$), and poly(vinyl pyrrolidone) were purchased from Sigma-Aldrich (Germany). The other chemicals that we used were analytical grade. White granules of film-grade HDPE resin for bag production was provided by Union J. Plus Co., Ltd. (Thailand). Luria–Bertani, Mueller–Hinton II broth powder, and Sueoka's high-salt media were obtained from Sigma-Aldrich (Singapore).

Bacterial Samples. *E. coli* DH5α was obtained from Novagen. *B. subtilis* BCC 6327 was purchased from BIOTEC Culture Collection (Bangkok, Thailand), and *S. typhimurium* was a gift from the Institute of Biotechnology, Vietnam Academy of Science and Technology.

Methods

Synthesis of the AgNP Traps. The AgNPs were synthesized and characterized by chemical reduction with poly(vinyl pyrrolidone) as a colloidal stabilizer with the method described by Dumri and Anh.[24] For AgNP trap fabrication, a 50-mL volume of colloidal AgNP solution was mixed with 250 mL of toluene, and the mixture was heated at 75°C for 45 min under vigorous stirring. After this, the AgNPs were located in the toluene phase, where they were present as an upper black layer in the reaction mixture. This black layer was collected though a 500-mL separatory funnel. Then, 5 g of PE granules was added, and the mixture was heated at 100°C for 25 min, during which the PE granules melted completely. The mixture was then ultrasonicated for a further 45 min at the same temperature, and afterward, the liquid mixture was cast in aluminum round trays 5 cm in diameter and approximately 5 mm in thickness [Figure 1(a)]. The trays were kept at an ambient temperature of 30°C for 12 h in a ventilating fume hood cabinet to evaporate the toluene completely. Dry, white, solid, round discs 1 mm in thickness (described here as AgNP traps) formed; these contained a high amount of AgNPs. Each final AgNP trap contained approximately 50 mg of AgNPs.

Synthesis of the PE/AgNP Nanocomposites. An appropriate number of AgNP traps were weighed first, ground into a mild powder, mixed with 50 g of PE granules at different ratios, and then finally blended in an internal mixer (Haake Rheomix Lab Mixers 610, Germany) at 60 rpm and 170°C for 8 min to extrude the final PE/AgNP nanocomposites with three different amounts of AgNPs at $\pm 5 \times 10^{-3}$, 5×10^{-4}, and 5×10^{-5} wt %. These samples were designated in this study as PE/AgNPs 5×10^{-3}, PE/AgNPs 5×10^{-4}, and PE/AgNPs 5×10^{-5}, respectively. These nanocomposites were cooled to ambient temperature and were used to fabricate discs 30 cm in diameter and 2 mm in thickness [Figure 1(b)] by a compression-molding machine (Toyo Seiki, Japan) at 180°C with 160 kg/cm^2 of pressure. PE discs without AgNPs were prepared as the control.

Characterization of the PE/AgNP Nanocomposites

Morphological Analysis by Transmission Electron Microscopy (TEM). The size of the AgNPs and their dispersal in the PE/AgNP nanocomposites were analyzed by TEM (JEM 1010, JEOL, Japan) at 80-kV operation (resolution = 3 Å). Ultrathin PE/AgNP specimens with a thickness of about 80 nm were cut by glass blades with an ultramicrotome Ultracut E (Leica, Germany) at −130°C in liquid nitrogen to prevent the deformation of the samples.

Mechanical Property Measurement. The tensile strength and elongation at break were measured according to ASTM D 638. The Young's modulus was measured according to DIN 53503 with a universal tensile tester (Zwick Z 2.5, Zwick GmbH & Co, Ulm, Germany) at a crosshead speed of 50 mm/min. Dumbbell-shaped specimens were prepared with dimensions of 9×1.2 mm^2 with a thickness of about 2 mm, a distance between shoulders of 4.5 cm, and a gauge length of 2.5×0.5 cm^2.

Differential Scanning Calorimetry (DSC). DSC measurements were carried out with a DSC 7 (PerkinElmer). Specimens of approximately 10 mg of different PE/AgNP samples were cut

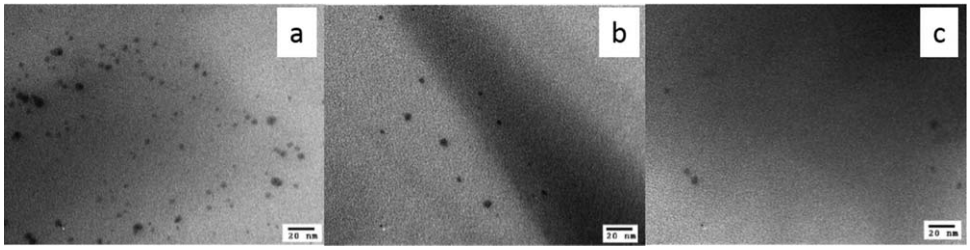

Figure 2. TEM micrographs of the PE/AgNP nanocomposites: (a) 5×10^{-3}, (b) 5×10^{-4}, and (c) 5×10^{-5} wt %.

and kept at room temperature for 10 min before heat treatment. Each sample was heated to 170°C with a 10°C/min heating step for 3 min. It was then cooled at 10°C/min to 25°C and maintained at this temperature for 3 min. The temperature of the sample was then raised to 170°C with a 10°C/min heating step. These second cooling step and third heating step were run to melt the crystalline content in the sample completely and to discard the thermal history of the first run. The T_m, T_c, heat of fusion (ΔH_f), and heat of crystallization of the nanocomposite samples were obtained from the thermograms. The crystallinities of the samples were calculated from the ratio of the ΔH_f values to the reference value of 100% crystallization HDPE from the following formula:

$$C \text{ of PE/AgNPs}(\%) = \frac{\delta H_f \text{ of PE/AgNPs}}{\delta H_f \text{ of 100\% HDPE}}$$

where C is percentage crystallinity of the PE/AgNP samples and ΔH_f of 100% HDPE was the reference value of 100% crystalline HDPE (293 J/g).[25]

Influence of the PE/AgNP Nanocomposites on the Lag–Log Phases of the Bacterial Growth Rate

Preparation of the Materials. ***Media for the tested bacteria.*** *E coli* and *S. typhimurium* were cultured in Luria–Bertani and Mueller–Hinton II broth media, respectively. *B. subtilis* was grown in a high-salt medium (665 mL of distilled water, 100 mL of 10 × Spizizen's salt, 25 mL of 20% w/v glucose, 50 mL of 0.1% w/v L-tryptophan, 10 mL of 2% w/v casein, 50 mL of 10% w/v yeast extract, 100 mL of 8% w/v arginine, and 0.4% w/v of histidine).

Precultures of the tested bacteria. A volume of 100 µL of stock culture in glycerol of each bacterium was pipetted into 3 mL of a compatible liquid medium in a 15-mL test tube and shaken overnight at 200 rpm and 37°C. Afterward, a 500-µL aliquot of preculture was inoculated into 100 mL of a compatible medium in a 500-mL Erlenmeyer flask and shaken at 200 rpm and 37°C until the OD_{600} absorbance value reached 0.1. These precultures were used promptly for bacterial grow rate testing.

Preparation of PE/AgNP samples for bacterial growth rate testing. The PE/AgNPs and the PE discs used as controls were cut into square pieces with dimensions of 1×1 cm^2 [Figure 1(b)], washed with acetone to remove all impurities on the surface, and autoclaved at 121°C for 20 min before use.

Monitoring of the Bacterial Lag–Log Growth Phases in the Presence of the PE/AgNP Nanocomposites. The monitoring test for the evaluation of the bacterial growth was adapted from the procedure in ASTM E 2149-10. Ten square pieces of autoclaved PE/AgNP nanocomposites or PE were placed into each 100-mL bacterial preculture in a 500-mL Erlenmeyer flask (as described previously) in which the OD_{600} had reached 0.1, and shaking was continued at 200 rpm and 37°C [Figure 1(c)]. From this point in time, the OD_{600} value of each bacterial culture was monitored every 30 min until it reached 2.0. The relative OD_{600} values were standardized to evaluate the influence of the PE/AgNP nanocomposites on the growth rate of the bacteria. Mixed bacterial cultures with neat PE square pieces and pure bacterial cultures were used as controls.

RESULTS AND DISCUSSION

Characterization of the PE/AgNP Nanocomposites

TEM Analysis. Typical surfaces of the three types of PE/AgNP nanocomposites with AgNP contents of 5×10^{-3}, 5×10^{-4}, and 5×10^{-5} wt % were analyzed by TEM, as shown in Figure 2(a–c), respectively. Five random samples of each PE/AgNP nanocomposite (i.e., with AgNP contents of 5×10^{-3}, 5×10^{-4}, and 5×10^{-5}) were chosen for analysis, and their TEM images revealed that (1) the AgNP distributions on all of the PE/AgNP surfaces were generally uniform (Figure 2), and (2) at the same magnification (100,000×), the AgNP densities on the surfaces of the samples followed the order PE/AgNPs 5×10^{-3} > PE/AgNPs 5×10^{-4} > PE/AgNPs 5×10^{-5} (Figure 2). The uniform distribution of the AgNPs on the surfaces of these PE/AgNP nanocomposites met the uniformity requirement for the further production of field testing bags. The TEM images showed that the sizes of the AgNPs ranged from approximately 2 to 20 nm, and the densities of the AgNPs in these PE/AgNP nanocomposites were proportional to the AgNP content. Figure 2(a) shows the significantly higher density of the AgNPs at 5×10^{-3} wt %, whereas the densities of the AgNPs at 5×10^{-4} [Figure 2(b)] and 5×10^{-5} wt % [Figure 2(c)] were obviously lower. The agglomeration of AgNPs in these PE/AgNP nanocomposites was not observed. However, in some previous research, AgNPs agglomerated during the synthesis of chitosan and poly(styrene-*co*-acrylic acid) or ceramsite nanocomposites.[26–28] In this study, the practical synthesis of AgNPs, according to our previous work (Dumri *et al.*[24]), prevented the agglomeration of AgNPs (data not shown). The AgNPs were captured in the PE matrix to mold AgNP traps with given sizes and with quantitative amounts of AgNPs. The ground AgNP traps were mixed with raw PE granules to form PE/AgNP nanocomposites. Noticeably, two solid phases could be mixed well, and they may have contributed to the uniform dispersion of AgNPs in the PE matrix (Figure 2).

The introduction of AgNPs into a certain plastic matrix can be performed by diverse methods, from loading techniques to the control of the weight ratios between the raw plastic material and AgNPs. In previous reports, AgNPs in a toluene mixture were added directly into the *in situ* polymerization of ethylene. However, TEM analysis showed clusters of AgNPs on the surface of the end product.[19] SiO_2/AgNP and TiO_2/AgNP complexes were synthesized as AgNP carriers and mixed with melting LDPE and extruded to a plain film.[18] Eventually, AgNPs were agglomerated in the matrix because the AgNPs were first deposited on the SiO_2 and TiO_2 particle surfaces, and these particles tended to cluster in their colloidal solutions.[29,30] This AgNP agglomeration depressed their functional toxicity by reducing the release of Ag^+ ions[22,23]; this reduced the antibacterial properties of the relevant nanocomposites. In another study, an LDPE film was treated by corona air plasma to increase the adhesion of the AgNPs; then, the AgNPs were coated onto the LDPE film by the immersion of the film into an AgNP colloidal solution under continuous stirring and heating at 80°C. This technique, however, was sophisticated, and only AgNPs with a size of 70 nm were mounted on the film surface.[31] In terms of a bacterial killing agent, AgNPs were reported to kill both Gram-negative bacteria, such as *Acinetobacter, Escherichia, Pseudomonas, Salmonella*, and *Vibrio* species, and Gram-positive bacteria, such as *Bacillus, Clostridium, Enterococcus, Listeria, Staphylococcus*, and *Streptococcus* species.[32–38] The mechanism of bactericide by AgNPs is the bacterial toxicity of Ag^+ ions,[9,32] and a smaller AgNP size will release Ag^+ ions faster.[39,40] Hence, the PE/AgNP nanocomposites with AgNPs with diameters of 2–20 nm in this study were presumed to kill the selected bacteria in a similar manner to AgNPs with diameters in the range 3–30 nm, as previously reported.[41,42]

Mechanical and Thermal Properties

The tensile strength of the neat PE was determined to be approximately 25.8 ± 1.7 MPa and was slightly higher than the tensile strengths of the PE/AgNPs 5×10^{-5}, 5×10^{-4}, and 5×10^{-3}; these values were 24.9 ± 2.0, 23.8 ± 2.2, and 23.1 ± 1.8 MPa, respectively [Figure 3(a)]. The elongation at break of the neat PE was 113.9 + 13.0%, whereas its values were 109.7 ± 20.0, 99.2 ± 15.0, and $96.6 \pm 17.9\%$ for PE/AgNPs 5×10^{-5}, 5×10^{-4}, and 5×10^{-3}, respectively [Figure 3(b)]. Figure 3(c) presents the Young's modulus values of the neat PE and PE/AgNPs 5×10^{-5}, 5×10^{-4}, and 5×10^{-3} of 200 ± 25.0, 151 ± 19.0, 170 ± 20.0, and 190 ± 22.0 MPa, respectively. Apparently, the addition of AgNPs at 5×10^{-5}, 5×10^{-4}, and 5×10^{-3} wt % in the PE/AgNP nanocomposites slightly reduced the tensile strength, elongation, and Young's modulus in comparison to neat PE. Figure 3(a,b) shows that the tensile strength and elongation at break of PE/AgNPs 5×10^{-5} were nearly equal to those of neat PE and were higher than those of PE/AgNPs 5×10^{-4} and 5×10^{-3}. On the other hand, the Young's modulus values of PE/AgNPs 5×10^{-3} were 10 and 20% higher than those of PE/AgNPs 5×10^{-4} and 5×10^{-5}, respectively [Figure 3(c)]. In this study, the incorporation of AgNPs into the PE matrix apparently decreased the homogeneity of the PE polymer. We assumed that the AgNPs disrupted the PE molecular interaction and led to a decrease in the tensile strength and elongation of the PE/AgNP nanocomposites as the AgNP concentration increased [Figure 3(a,b)]. However, the AgNPs could hypothetically bond with the PE molecules via

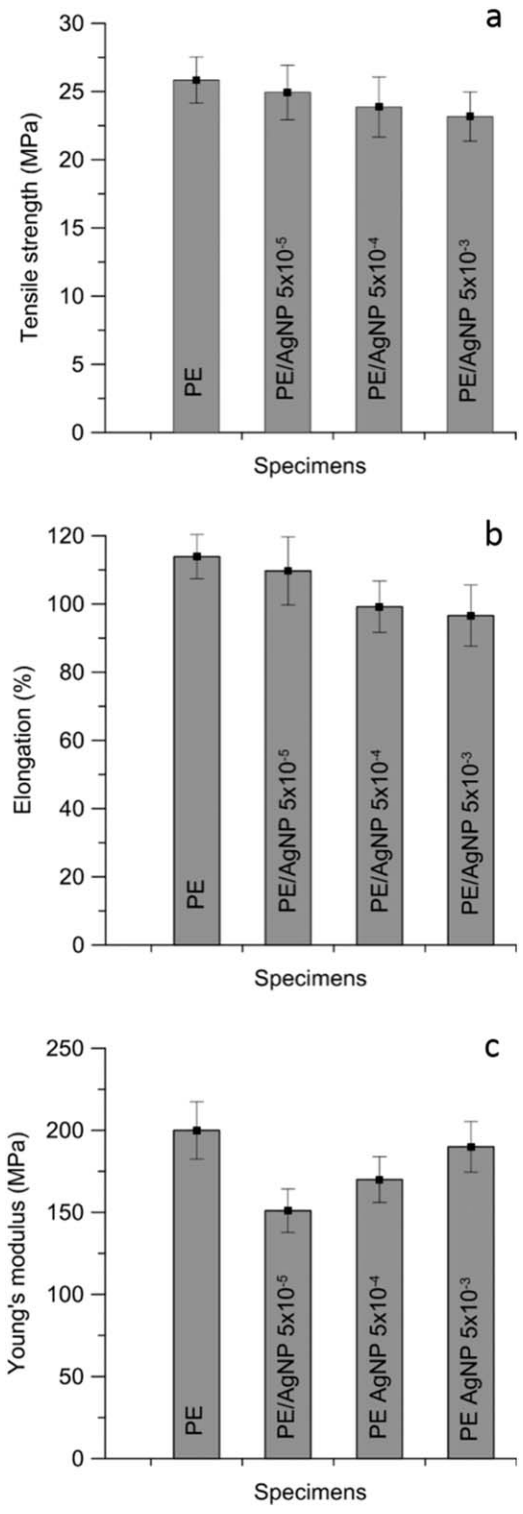

Figure 3. (a) Tensile strength, (b) elongation at break, and (c) Young's modulus values of the PE and different PE/AgNP nanocomposites. The data points represent the means of five measurements (standard deviation < 10%).

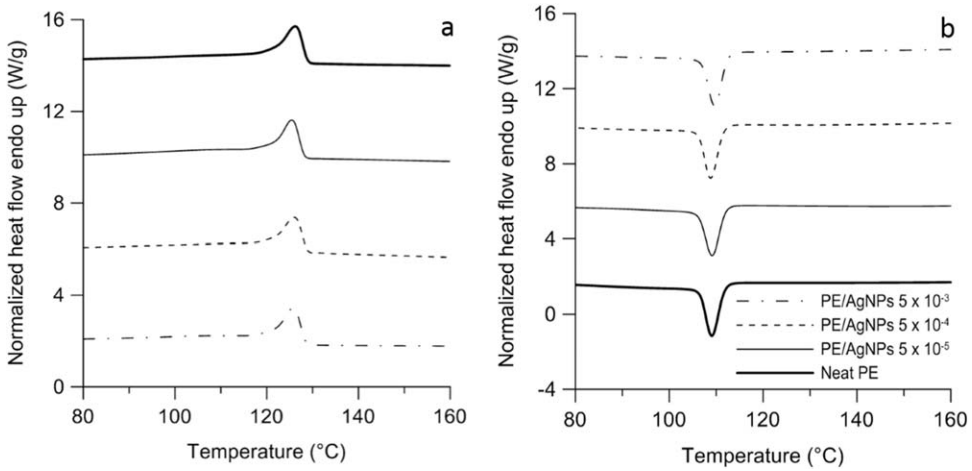

Figure 4. DSC thermograms of the PE/AgNP nanocomposites and neat PE. The thick, black line represents neat PE. The thin, dotted, and dashed–dotted lines represent the PE/AgNP nanocomposites with concentrations of 5×10^{-5}, 5×10^{-4}, and 5×10^{-3} wt %, respectively.

possible intermolecular forces; for example, Van der Waals forces and these bonds might have transferred applied stress and energy between the PE molecules and the AgNPs. Hence, this might have contributed to the increase in the Young's modulus of the PE/AgNP nanocomposites [Figure 3(c)] when the concentration or density of AgNPs increased. In addition, the decrease in the crystallinity after the incorporation of AgNPs into the PE matrix (discussed later) might have also contributed to the decrease in the tensile strength and the increase in Young's modulus. Overall, AgNP contents in the range 5×10^{-5} to 5×10^{-3} wt % of the bulk PE influenced the tensile strength and elongation at break. However, these values were comparable to those of common PE plastic.[43] Therefore, these PE/AgNP nanocomposites are expected to be usable in food packaging applications.

Typical thermograms for the PE/AgNP nanocomposites and neat PE samples are shown in Figure 4. The T_m values of the different PE/AgNP nanocomposites and neat PE were similar at 126 ± 0.5°C. The T_c values of the PE/AgNP nanocomposites and neat PE were also similar, but at 109 ± 0.6°C. This revealed that the addition of AgNPs at 5×10^{-5}, 5×10^{-4}, and 5×10^{-3} wt % at AgNP diameters of 2–20 nm did not change the behavior of the PE matrix in terms of T_m and T_c. On the other hand, the peak areas representing ΔH_f for PE/AgNPs 5×10^{-5} and 5×10^{-4} were both 5% lower, and the value for PE/AgNPs 5×10^{-3} was 7% lower in comparison to that of neat PE without AgNPs (Figure 5). The crystallinity of neat PE was 51%, whereas the crystallinity was 48% for both PE/AgNPs 5×10^{-5} and 5×10^{-4}, and it was 46% for PE/AgNPs 5×10^{-3}. These values reflected the influence of the AgNP content on the crystallinity of the PE/AgNP nanocomposites. Herein, the higher AgNP content in the PE/AgNP nanocomposites lowered the crystallinity. This phenomenon was in agreement with studies

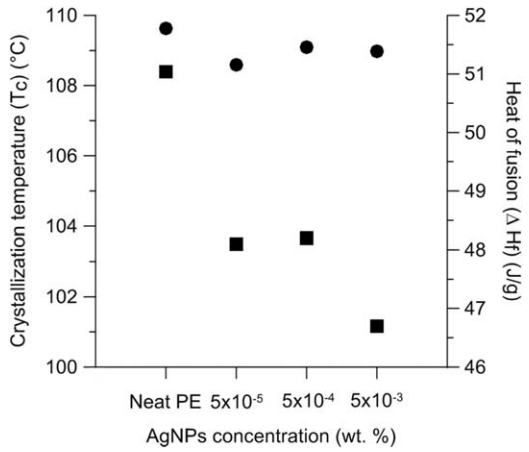

Figure 5. Influence of the AgNP concentration on the (●) T_c and (■) ΔH_f values of the PE/AgNP nanocomposites and neat PE. The value of ΔH_f was normalized to the AgNP concentrations. The data points represent the means of five measurements (standard deviation < 10%).

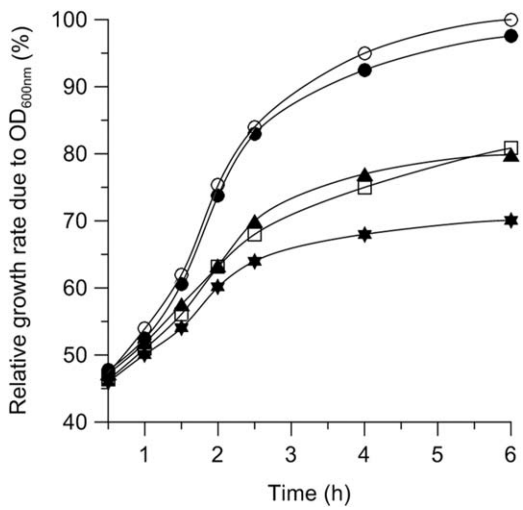

Figure 6. Influence of the PE/AgNP nanocomposites on the growth rate of the *E. coli* liquid cultures: (◯) pure *E. coli*, (●) mixed cultures with PE, (□) mixed cultures with PE/AgNP nanocomposites (5×10^{-5} wt %), (▲) mixed cultures with PE/AgNP nanocomposites (5×10^{-4} wt %), and (★) mixed cultures with PE/AgNP nanocomposites (5×10^{-3} wt %). The data points represent the means of three cultures (standard deviation < 15%).

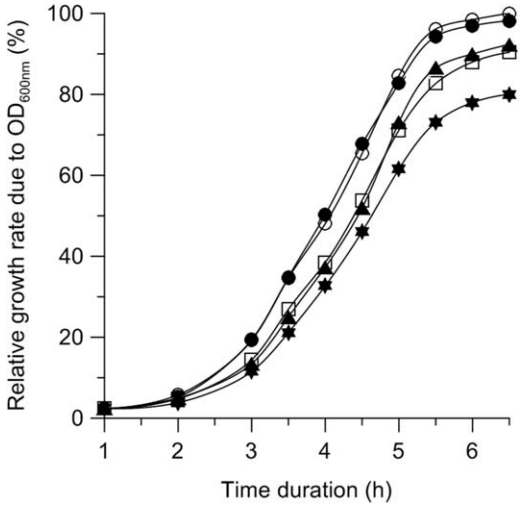

Figure 7. Influence of the PE/AgNP nanocomposites on the growth rate of the *B. subtilis* liquid cultures: (◯) pure *B. subtilis*, (●) mixed cultures with PE, (□) mixed cultures with PE/AgNP nanocomposites (5×10^{-5} wt %), (▲) mixed cultures with PE/AgNP nanocomposites (5×10^{-4} wt %), and (★) mixed cultures with PE/AgNP nanocomposites (5×10^{-3} wt %). The data points represent the means of three cultures (standard deviation < 15%).

where the AgNP content was varied in other types of PE and poly(vinylidene fluoride)/AgNP nanocomposites.[19,44,45]

Influence of the PE/AgNP Nanocomposites on the Lag–Log Phase Growth of the Tested Bacteria

Bacterial precultures were prepared with the aim of generating the subcultures of bacterial populations in a large scale in the lag phase so that the number of bacterial cells was constant before the log phase or exponential growth phase.[46] By this means, the growth rate of the bacterial cultures due to the presence of PE/AgNP nanocomposites was evaluated accurately over time. The OD_{600} values in the range 0.1–2.0 for cell densities of *E. coli, B. subtilis*, and *S. typhimurium* cultures indicated the bacterial growth rates.

In the case of *E. coli* cultures, the growth rates after 1 h began to be differentiated (Figure 6). The log phase of the pure cultures and the mixed cultures with neat PE occurred exponentially and were clearly higher than those of all of the other mixed cultures with PE/AgNP nanocomposites during cultivation. The mixed cultures with neat PE had similar growth rates as pure cultures, and only a minor difference of 3% was observed after 6 h. The growth rate of mixed cultures with PE/AgNPs 5×10^{-3} reached 70% after 6 h, whereas the growth rate was 80% for the mixed cultures with PE/AgNPs 5×10^{-4} and 5×10^{-5}. The growth rates in the mixed cultures with PE/AgNPs 5×10^{-4} and 5×10^{-5} were almost similar during 6 h of cultivation and 10% higher in comparison to the mixed cultures with PE/AgNPs 5×10^{-3}.

In the case of *B. subtilis* cultures (Figure 7), the log phases of the pure cultures and mixed cultures with neat PE were 20% after 3 h of cultivation, whereas this was 10% in the cases of mixed cultures with PE/AgNPs 5×10^{-3} and both PE/AgNPs 5×10^{-4} and 5×10^{-5}. The growth rates of the pure cultures and mixed cultures with neat PE were almost identical at all of the sampling time points and differed only approximately 2% at the end point (after 7 h) of cultivation. The growth rates of the cultures were 80 and 90% after 7 h in the presence of PE/AgNPs 5×10^{-3} and both PE/AgNPs 5×10^{-4} and 5×10^{-5}, respectively. Bacterial growth was similarly restricted in the presence of PE/AgNPs 5×10^{-4} and 5×10^{-5}.

In the case of the *S. typhimurium* cultures (Figure 8), the log-phase curves of the pure cultures and mixed cultures with neat PE almost coincided. The log-phase curves of the mixed cultures with the PE/AgNP nanocomposites and pure culture started to separate after 6 h of cultivation. The log-phase curves of the mixed cultures with PE/AgNPs 5×10^{-4} and 5×10^{-5} were identical during 10 h of cultivation and the growth rates of relevant cultures were similar. The growth rate of the mixed bacterial cultures with PE/AgNPs 5×10^{-3} and both PE/AgNPs 5×10^{-4} and 5×10^{-5} were 70 and 90%, respectively. The mixed cultures with PE/AgNPs 5×10^{-4} and 5×10^{-5} had growth rates that were 20% higher than those of the mixed culture with PE/AgNPs 5×10^{-3} after 10 h of cultivation.

In all of the mixed bacterial cultures with PE/AgNPs 5×10^{-3}, the growth rates in the lag–log phases were restricted 30% for both *E. coli* (Figure 6) and *S. typhimurium* (Figure 8) and 20% for *B. subtilis* (Figure 7) in comparison to the pure bacterial and mixed bacterial cultures with neat PE. By means of this, the AgNPs in the PE/AgNP nanocomposites revealed their antibacterial activity by killing bacterial cells in the early growth stages of bacteria. The lower restriction of *B. subtilis* (a Gram-positive bacterium) growth compared to those of *E. coli* and *S. typhimurium* (Gram-negative bacteria) was explained by the lower sensitivity of the *B. subtilis* to the AgNPs. This phenomenon was also observed in case of the poly(vinyl alcohol)/AgNP

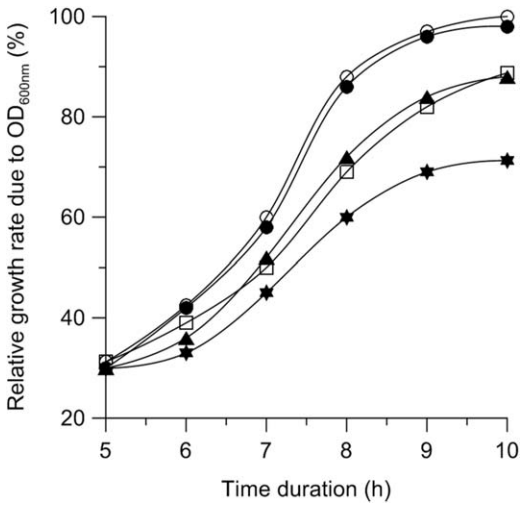

Figure 8. Influence of the PE/AgNP nanocomposites on the growth rate of the *S. typhimurium* liquid cultures: (◯) pure *S. typhimurium*, (●) mixed cultures with PE, (□) mixed cultures with PE/AgNP nanocomposites (5×10^{-5} wt %), (▲) mixed cultures with PE/AgNP nanocomposites (5×10^{-4} wt %), and (★) mixed cultures with PE/AgNP nanocomposites (5×10^{-3} wt %). The data points represent the means of three cultures (standard deviation < 15%).

nanocomposites, which showed a moderate antibacterial activity to *B. subtilis* in comparison to *E. coli*.[47] In general, the Gram-positive *B. sublitis* has a thick peptidoglycan cell wall, and it has evolved as a protective mechanism against antibiotics.[48] This cellular structure might have been a factor in our study. Although the production technique of the other PE/AgNP types were different, those other nanocomposites also showed antibacterial activity to both Gram-positive bacteria, such as *Bacillus* species, *Listeria monocytegenes*, and *Staphylococcus aureus*,[13,31] and Gram-negative bacterial, such as *E. coli* and *Klebsiella pneumoniae*.[19,49]

In this study, all of the PE/AgNP nanocomposites (i.e., 5×10^{-3}, 5×10^{-4}, and 5×10^{-5}) showed significant antibacterial activity during the early growth stage or lag–log phases of the tested bacteria. The immersion of PE/AgNP square pieces into the fresh bacterial liquid cultures under shaking conditions was assumed to enhance the contact between the bacterial cells and the AgNPs. Therefore, the suicidal probability of the cells was higher. In much previous research, antibacterial activity tests for various nanocomposites were performed on agar plate cultures or immobilized cultures. Antibacterial evaluations, including those of *E. coli, Bacillus* species, and *Salmonella* species, were carried out on the basis of the size of the bacterial inhibition zones after an average time of 24 h or even 72 h.[19,50–52] Herein, the restriction of *E. coli* (Figure 6), *B. subtilis* (Figure 7), and *S. typhimurium* (Figure 8) was noticed after 1.5, 3, and 6 h, respectively. In terms of antibacterial packaging applications, this may have been significant for the early prevention of certain pathogenic bacteria with AgNP-containing nanocomposites. High amounts of AgNPs at 5 and 9 wt % in other related PE and poly(3-hydroxybutyrate-*co*-4-hydroxybutyrate)/chitosan nanocomposites prevented *E. coli* growth up to 99% in comparison to the neat PE after 24 h.[19,53] *Salmonella* and *Bacillus* species were strongly inhibited in the presence of AgNP with an amount of approximately 1.2 wt % in a gelatin film and epoxy/clay nanocomposites.[51,52] Our results show that AgNPs at 5×10^{-3} wt % obviously restricted the growth of *E. coli, B. subtilis*, and *S. typhimurium* by 30% after 6, 7, and 10 h of cultivation, respectively. A poly(vinyl alcohol)/AgNP nanocomposite containing similarly sized AgNPs (19 nm) and with an AgNP concentration of 4×10^{-3} wt % also strongly inhibited *S. aureus* and *E. coli*.[47] At the same concentration (2 wt %) in a polysulfone membrane for wastewater filtration, embedded AgNPs 30 nm in diameter were reported to inhibit the growth of *E. coli* more effectively than AgNPs 70 nm in diameter.[54] Work elsewhere showed that large AgNPs (80 nm) could kill *E. coli* but at high concentrations, for example, 2 wt % in HDPE composites.[55] The lower amounts of AgNPs used here (5×10^{-4} and 5×10^{-5} wt %) also demonstrated antibacterial activity. Other cellulose/AgNP nanocomposites also revealed antibacterial activity at 5×10^{-4} wt % AgNPs to both Gram-positive *B. subtilis* and other Gram-negative *K. pneumoniae*.[56] Natural rubber composites containing 6×10^{-4} wt % AgNPs 20 nm in diameter enhanced the antibacterial activity to *E. coli* and *S. aureus*.[57] The availability of AgNPs to kill bacteria at low concentrations might be significant due to the use of AgNPs (although they kill food and waterborne bacteria); however, they may cause oxidative stress that effects respiration rate of experimental vertebrate organisms, such as zebra fish and mouse embryos.[23,58,59]

CONCLUSIONS

The fabrication of PE/AgNP nanocomposites with preparative AgNP traps was simple, reproducible, and not time consuming and could prevent the agglomeration of AgNPs on the material surface. The capture of AgNPs in compact PE traps brought to the PE/AgNP production the following advantages: (1) a reduction in the agglomeration of AgNPs, which restricted the antibacterial activity of the AgNPs via the release of Ag^+; (2) the enhancement of the uniform distribution and control of the amount of AgNPs in the final PE/AgNP nanocomposites; and (3) the facilitation of the mixing between the raw PE granules and the AgNPs because both were dry PE fractions.

The use of the AgNP trap pattern could be applied for other nanocomposite type fabrications to enhance their possible antibacterial activity with AgNPs. Because the agglomeration of AgNPs on the PE/AgNP surface was prevented, the functional AgNPs revealed effective antibacterial activities. Herein, the PE/AgNP nanocomposites restricted common pathogenic bacteria in their early developmental stage. On the other hand, the addition of AgNPs at low concentrations only slightly changed the mechanical properties of the used commercial PE. With these factors taken into account, these PE/AgNP nanocomposites are highly promising for active packaging applications and production, especially for low-income areas.

ACKNOWLEDGMENTS

The authors gratefully acknowledge the receipt of a postdoctoral fellowship in 2015 from Chiang Mai University and its financial support.

REFERENCES

1. Lansdown, A. B. *Curr. Prob. Dermatol.* **2006**, *33*, 17.
2. Palza, H. *Int. J. Mol. Sci.* **2015**, *16*, 2099.
3. Chretien, J. P.; Anyamba, A.; Small, J.; Britch, S.; Sanchez, J. L.; Halbach, A. C.; Tucker, C.; Linthicum, K. J. *PLoS Curr.* **2015** Jan 26, 7.
4. Anyamba, A.; Chretien, J. P.; Small, J.; Tucker, C. J.; Linthicum, K. J. *Int. J. Health Geogr.* **2006**, *5*, 60.
5. Chaturongkasumrit, Y.; Techaruvichit, P.; Takahashi, H.; Kimura, B.; Keeratipibul, S. *Sci. Total Environ.* **2013**, *463*, 959.
6. Chua, K. B. *Malays. J. Pathol.* **2010**, *32*, 75.
7. Torti, J. *J. Glob. Health* **2012**, *2*, 020304.
8. Kumar, R.; Münstedt, H. *Biomaterials* **2005**, *26*, 2081.
9. Reidy, B.; Haase, A.; Luch, A.; Dawson, K.; Lynch, I. *Materials* **2013**, *6*, 2295.
10. Gambino, M.; Marzano, V.; Villa, F.; Vitali, A.; Vannini, C.; Landini, P.; Cappitelli, F. *J. Appl. Microbiol.* **2015**, *118*, 1103.
11. Greulich, C.; Kittler, S.; Epple, M.; Köller, M. *Langenbecks Arch. Surg.* **2009**, *394*, 495.

12. Pauksch, L.; Hartmann, S.; Rohnke, M.; Szalay, G.; Alt, V.; Schnettler, R.; Lips, K. S. *Acta Biomater.* **2014**, *10*, 439.
13. Tamayo, L. A.; Zapata, P. A.; Vejar, N. D.; Azócar, M. I.; Gulppi, M. A.; Zhou, X.; Thompson, G. E.; Rabagliati, F. M.; Páez, M. A. *Mater. Sci. Eng.* **2014**, *40*, 24.
14. Deng, Z.; Zhu, H.; Peng, B.; Chen, H.; Sun, Y.; Gang, X.; Jin, P.; Wang, J. *ACS Appl. Mater. Interfaces* **2012**, *4*, 5625.
15. Marini, M.; Niederhausern, S.; Iseppi, R.; Bondi, M.; Sabia, C.; Toselli, M.; Pilati, F. *Biomacromolecules* **2007**, *8*, 1246.
16. Wu, J. J.; Lee, G. J.; Chen, Y. S.; Hu, T. L. *Curr. Appl. Phys.* **2012**, *12*, S89.
17. Sung, S.-Y.; Sin, L. T.; Tee, T. T.; Bee, S. T.; Rahmat, A. R.; Rahman, W. A.; Tan, A. C.; Vikhraman, M. *Trends Food Sci. Technol.* **2013**, *33*, 110.
18. Becaro, A. A.; Puti, F. C.; Correa, D. S.; Paris, E. C.; Marconcini, J. M.; Ferreira, M. D. J. *Nanosci. Nanotechnol.* **2015**, *15*, 2148.
19. Zapata, P. A.; Tamayo, L.; Páez, M.; Cerda, E.; Azócar, I.; Rabagliati, F. M. *Eur. Polym. J.* **2011**, *47*, 1541.
20. Pourdanesh, F.; Jebali, A.; Hekmatimoghaddam, S.; Allaveisie, A. *Mater. Sci. Eng.* **2014**, *40*, 382.
21. Jang, M. W.; Kim, J. Y.; Ihn, K. J. *J. Nanosci. Nanotechnol.* **2007**, *7*, 3990.
22. Bae, E.; Lee, B. C.; Kim, Y.; Choi, K.; Yi, J. *Korean J. Chem. Eng.* **2013**, *30*, 364.
23. Gliga, A. R.; Skoglund, S.; Wallinder, I. O.; Fadeel, B.; Karlsson, H. L. *Part. Fibre Toxicol.* **2014**, *11*, 11.
24. Dumri, K.; Anh, D. H. *Enzyme Res.* **2014**, *9*, 389739.
25. Wunderlich, B. Macromolecular Physics; Academic: New York, **1973**; Vol. *1*.
26. Youssef, A. M.; Abdel-Aziz, M. S.; El-Sayed, S. M. *Int. J. Biol. Macromol.* **2014**, *69*, 185.
27. Song, C.; Chang, Y.; Cheng, L.; Xu, Y.; Chen, X.; Zhang, L.; Zhong, L.; Dai, L. *Mater. Sci. Eng.* **2014**, *36*, 146.
28. Qiu, S.; Huang, X.; Xu, S.; Ma, F. *Appl. Biochem. Biotechnol.*, to appear.
29. Gu, G.; Xu, J.; Wu, Y.; Chen, M.; Wu, L. *J. Colloid Interface Sci.* **2011**, *359*, 327.
30. Amin, S. A.; Pazouki, M.; Hosseinnia, A. *Powder Technol.* **2009**, *196*, 241.
31. Dehnavi, A. S.; Aroujalian, A.; Raisi, A.; Fazel, S. *J. Appl. Polym. Sci.* **2013**, *127*, 1180.
32. Wijnhoven, S. W. P.; Peijnenburg, W. J. G. M.; Herberts, C. A.; Hagens, W. I.; Oomen, A. G.; Heugens, E. H. W.; Roszek, B.; Bisschops, J.; Gosens, I.; Van De Meent, D.; Dekkers, S.; De Jong, W. H.; van Zijverden, M.; Sipsand, A. J. A. M.; Geertsma, R. E. *Nanotoxicology* **2009**, *3*, 109.
33. Yin, H. Q.; Langford, R.; Burrell, R. E. J. *Burn Care Rehabil.* **1999**, *20*, 195.
34. Percival, S. L.; Bowler, P. G.; Dolman, J. *Int. Wound J.* **2007**, *4*, 186.
35. Wright, J. B.; Lam, K.; Burrell, R. E. *Am. J. Infect. Control* **1998**, *26*, 572.
36. Baker, C.; Pradhan, A.; Pakstis, L.; Pochan, D. J.; Shah, S. I. J. *Nanosci. Nanotechnol.* **2005**, *5*, 244.
37. Morones, J. R.; Elechiguerra, J. L.; Camacho, A.; Holt, K.; Kouri, J. B.; Ramirez, J. T.; Yacaman, M. J. *Nanotechnology* **2005**, *16*, 2346.
38. Panacek, A.; Kvitek, L.; Prucek, R.; Kolar, M.; Vecerova, R.; Pizurova, N.; Sharma, V. K.; Nevecna, T.; Zboril, R. *J. Phys. Chem. B* **2006**, *110*, 16248.
39. Liu, J.; Sonshine, D. A.; Shervani, S.; Hurt, R. H. *ACS Nano* **2010**, *4*, 6903.
40. Lubick, N. *Environ. Sci. Technol.* **2008**, *42*, 8617.
41. Shahverdi, A. R.; Fakhimi, A.; Shahverdi, H. R.; Minaian, S. *Nanomedicine* **2007**, *3*, 168.
42. Agnihotri, S.; Mukherji, S.; Mukherji, S. *RSC Adv.* **2014**, *4*, 3974.
43. Rhim, J. W.; Wang, L. F.; Hong, S. I. *Food Hydrocolloids* **2013**, *33*, 327.
44. Jouni, M.; Boudenne, A.; Boiteux, G.; Massardier, V.; Garnier, B.; Serghei, A. *Polym. Compos.* **2013**, *34*, 778.
45. Manna, S.; Batabyal, S. K.; Nandi, A. K. *J. Phys. Chem. B* **2006**, *110*, 12318.
46. Rolfe, M. D.; Rice, C. J.; Lucchini, S.; Pin, C.; Thompson, A.; Cameron, A. D. S.; Alston, M.; Stringer, M. F.; Betts, R. P.; Baranyi, J.; Peck, M. W.; Hinton, J. C. D. *J. Bacteriol.* **2012**, *194*, 686.
47. Mahmoud, K. H. *Spectrochim. Acta A* **2015**, *138*, 434.
48. Silhavy, T. J.; Kahne, D.; Walker, S. *Cold Spring Harb. Perspect. Biol.* **2010**, *2*, a000414.
49. Lee, H. J.; Lee, S. G.; Oh, E. J.; Chung, H. Y.; Han, S. I.; Kim, E. J.; Seo, S. Y.; Ghim, H. D.; Yeum, J. H.; Choi, J. H. *Colloids Surf. B* **2011**, *88*, 505.
50. Liu, X.; Qi, S.; Li, Y.; Yang, L.; Cao, B.; Tang, C. Y. *Water Res.* **2013**, *47*, 3081.
51. Roy, B.; Bharali, P.; Konwar, B. K.; Karak, N. *Bioresour. Technol.* **2013**, *127*, 175.
52. Kanmani, P.; Rhim, J. W. *Food Chem.* **2014**, *148*, 162.
53. Rennukka, M.; Sipaut, C. S.; Amirul, A. A. *Biotechnol. Prog.* **2014**, *30*, 1469.
54. Mollahosseini, A.; Rahimpour, A.; Jahamshahi, M.; Peyravi, M.; Khavarpour, M. *Desalination* **2012**, *306*, 41.
55. Ziąbka, M.; Mertas, A.; Król, W.; Bobrowski, A.; Chłopek, J. *Macromol. Symp.* **2012**, *315*, 218.
56. Pinto, R. J.; Marques, P. A.; Neto, C. P.; Trindade, T.; Daina, S.; Sadocco, P. *Acta Biomater.* **2009**, *5*, 2279.
57. Zhang, Y.; Xue, X.; Zhang, Z.; Liu, Y.; Li, G. *J. Appl. Polym. Sci.* **2014**, *131*, 40746.
58. Bilberg, K.; Hovgaard, M. B.; Besenbacher, F.; Baatrup, E. J. *Toxicol.* **2012**, *29*, 3784.
59. Lee, Y. H.; Cheng, F. Y.; Chiu, H. W.; Tsai, J. C.; Fang, C. Y.; Chen, C. W.; Wang, Y. J. *Biomaterials* **2014**, *35*, 4706.